FUDMA Journal of Engineering and Technology
ISSN: 3092-9385
https://fjet.fudutsinma.edu.ng/index.php/fjet/
Volume 2, Issue 2, 2026, 61-70

Kinetic Modelling of Sonocatalytic Phenol Degradation over Alumina-Supported Copper Oxide Catalyst

Abdullahi YAHAYA[1*], Ahmad ADO[2], Jaju A. MUHAMMAD[3], Zaharaddeen G. SANI[4], Baba A. OLUWA[5], Abdulazeez A. YUSUF[6]

[1*,2,3]Chemical Engineering Department, Ahmadu Bello University, Zaria, Nigeria
[2]Dangote Fertilizer Limited, Ibeju-Lekki, Lagos, Nigeria
[4,5,6]National Research Institute for Chemical Technology, Basawa, Zaria, Nigeria

[1*]aylukman01@gmail.com, [2]ahmadado63@gmail.com, [3]muhjaju@yahoo.co.uk, [4]zaharaddeen@gmail.com, [5]olubababdul@gmail.com, [6]zeezoatta@gmail.com

Abstract

Phenol is a toxic organic pollutant often found in industrial wastewater, and its resistance to conventional treatment has made it a key target for advanced oxidation processes. In this study, a 9 wt% CuO/Al_2O_3 catalyst was prepared by incipient-wetness impregnation and evaluated for sonocatalytic phenol degradation in the presence of hydrogen peroxide. The catalyst was characterized using X-ray diffraction, nitrogen adsorption–desorption analysis, and scanning electron microscopy. The results confirmed the formation of CuO species on alumina, with preserved surface area, pore volume, and accessible surface morphology. Phenol degradation was investigated under ultrasound irradiation by varying H_2O_2 concentration, catalyst dosage, initial pH, and temperature. Sole sonolysis showed low degradation efficiency, reaching only about 8 % after 100 min. The addition of 9Cu/A and H_2O_2 greatly increased phenol removal, with optimal performance obtained at 30 mM H_2O_2, 20 g/L catalyst dosage, pH 4, and 70 °C. Excess H_2O_2 or catalyst loading lowered degradation due to radical scavenging and ultrasonic wave attenuation. Kinetic analysis showed that phenol degradation followed an apparent pseudo-first-order model, with a rate constant of approximately 0.0331 min^{-1} under optimal conditions, compared with about 0.0008 min^{-1} for sonolysis with H_2O_2 alone. The findings show that CuO/Al_2O_3 promotes H_2O_2 activation and strengthens sonochemical phenol oxidation.

Keywords: *Phenol degradation; CuO/Al_2O_3 catalyst; sonocatalysis; hydrogen peroxide; advanced oxidation process; pseudo-first-order kinetics; wastewater treatment; hydroxyl radical.*

1.0 Introduction

Phenol is a persistent organic pollutant (POP) commonly found in effluents from petroleum refining, petrochemical manufacturing, resin production, and other fine-chemical industries [1]. Its toxicity and resistance to conventional treatment processes make it a representative model compound for advanced oxidation studies [2]. Sonolysis is considered promising because acoustic cavitation generates localized hot spots that split water molecules and produce highly reactive radical species [3]. However, sonolysis alone is typically slow for hydrophilic and non-volatile molecules such as phenol [4], as these compounds remain predominantly in the liquid bulk rather than in the most reactive cavitation zones [5].

To address this limitation, ultrasound is frequently combined with an external oxidant and a heterogeneous catalyst [6]. An oxidant such as hydrogen peroxide (H_2O_2) provides an additional source of hydroxyl radicals, while a solid catalyst can accelerate H_2O_2 activation, generate interfacial reaction sites, and enhance local cavitation [3]. Among the various metal oxides investigated for wet oxidation and Fenton-like systems, copper oxide (CuO) has demonstrated strong activity against phenolic pollutants, particularly when dispersed on high-surface-area alumina (Al_2O_3) [1].

CuO/Al_2O_3 thus represents an attractive, iron-free catalyst platform for sonocatalytic oxidation. Alumina provides a large surface area and pore network for effective CuO dispersion, while copper oxide supplies the redox-active centers necessary for H_2O_2 decomposition [7]. Although previous studies have demonstrated that CuO-based catalysts can significantly enhance degradation efficiency, the intrinsic behavior of CuO/Al_2O_3 catalyst requires further investigation, as it establishes the kinetic activity baseline for evaluating the catalyst [8].

Previous research has shown that alumina-supported copper oxides are effective catalysts for phenol oxidation. Most studies, though, have focused on catalyst preparation, reaction conditions, product selectivity, and stability rather than on detailed kinetic analysis of the degradation process [5]. Jibril *et al.* (2013) found that alumina-supported copper oxides removed substantial amounts of phenol and total organic carbon (TOC) during microwave-assisted oxidation, and that copper loading and catalyst stability strongly affected performance [9]. Kim *et al.* (2007) also observed that the activity and mineralization selectivity of $CuOx/Al_2O_3$ increased with copper loading up to an optimal point, as copper species changed from isolated Cu^{2+} ions to well-dispersed clusters

Received: 06/06/2026; Revised: 21/07/2026; Accepted: 27/07/2026; Published: 13/08/2026

and then to bulk CuO at higher loadings [10]. More recently, Devard *et al.* (2019) showed that Cu/Al_2O_3 is highly active for phenol wet oxidation with H_2O_2, and that the calcination temperature affects Cu–Al–O interactions and copper leaching [1].

Detailed kinetic analysis has been performed for CuO/Al_2O_3-based phenol oxidation. However, it has usually been under very different conditions, such as supercritical water oxidation using Langmuir–Hinshelwood–Hougen–Watson and Mars–van Krevelen models [11], or in broader copper-based Fenton-type systems treating complex mixtures rather than just phenol [12]. Together, these studies show that CuO/Al_2O_3 is an important catalyst, but a clear gap remains in the kinetic modeling of phenol degradation over CuO/Al_2O_3 under sonocatalytic conditions. This study aims to fill that gap by examining phenol degradation over CuO/Al_2O_3 and evaluating a suitable kinetic model for the process.

2.0 Materials and Methods

2.1 Materials and apparatus

All reagents were of analytical grade and used as provided. Copper nitrate trihydrate served as the copper precursor, gamma-Al_2O_3 (γ-Al_2O_3) was the catalyst support, phenol was the model pollutant, and 30 wt% H_2O_2 functioned as the oxidant. Dilute acid and alkali solutions were used to adjust the pH, while deionized water was used in all preparations.

2.2 Catalyst preparations and characterization

A 9 wt% CuO/Al_2O_3 catalyst, designated as 9Cu/A, was prepared by incipient-wetness impregnation. Calculated amount of the copper precursor (corresponding to 9 wt% CuO/Al_2O_3 weight loadings) was dissolved in deionized water. γ-Al_2O_3 powder was then slowly added to the solution under stirring. The slurry was then evaporated to dryness at 70 °C. The resulting solid was dried at 110 °C for 12 h and calcined in air at 600 °C for 4 h.

The prepared catalysts were further characterized by X-ray diffraction (XRD) for the phase composition of the support and catalysts using a Philips PW1710 with CuKα radiation (λ = 1.5406 Å, 40 kV, 40 mA) at a scan rate (2θ) of 0.02 s^{-1}. Textural properties (specific surface area (m^2/g), average pore diameter (nm), and BJH pore volumes (cm^3/g)) were obtained from N_2 adsorption–desorption at 77 K using a Micromeritics ASAP 2020 instrument. The Brunauer–Emmett–Teller (BET) method was used to determine surface area, and the BJH method was used to determine pore size. Morphology and particle dispersion were examined by scanning electron microscopy (SEM) on a JEOL JSM-840A microscope.

2.3 Degradation procedure

Phenol degradation experiments were carried out in an ultrasonic bath (Soniclean PS-40A) operating at 40 kHz and 240 W. The bath had a maximum heating capacity of 300 W. In a typical run, 50 mL of an aqueous phenol solution (25 mg/L) was placed in a glass reactor, and the temperature was set to the desired set point (50, 60, or 70 °C). The catalyst (pre-dried) was added to achieve the desired loading (expressed in g/L). The initial pH of the solution was adjusted by adding dilute HCl or NaOH. The reactor was covered to minimize evaporation. The reaction mixture was irradiated with ultrasound under constant conditions. Representative samples (2–3 mL) were withdrawn, centrifuged (6,000 rpm, 10 min) to remove solids (catalyst particles), and UV–Vis spectrophotometry at λ = 270 nm to determine phenol concentration.

The experimental variables were studied using a sequential one-factor-at-a-time approach (OFAT). First, the effect of sole sonolysis for 100 min, followed by a combination of sonolysis with catalyst (20 g/L 9Cu/A) in the absence of H_2O_2, then the concentration of H_2O_2 was tested by adding 0–50 mM H_2O_2 to the phenol solution (pH 6.3, 20 g/L catalyst, 50 °C). Next, at 50 °C and pH 6.3, the catalyst loading was varied from 0 to 28 g/L (at 30 mM H_2O_2) for 100 min. Then the effect of initial pH was examined by varying pH from 3 to 6 (at 50 °C, 20 g/L catalyst, 30 mM H_2O_2, 100 min). Finally, the temperature was varied (50, 60, 70 °C) at pH 4, 20 g/L, 30 mM H_2O_2, 100 min. Each experiment was repeated at least three times to ensure reproducibility.

2.4 Kinetic analysis

To enable a consistent comparative kinetic metric, the 100-minute results were analyzed using an apparent pseudo-first-order model.

$$kapp = -\left(\frac{1}{t}\right) ln\left(\frac{C_t}{C_0}\right) \quad (1)$$

where C_0 and C_t are the initial and final phenol concentrations, respectively, and t = 100 min for the endpoint experiments. This approach is designed as a practical comparative model for process intensification rather than a comprehensive mechanistic rate law.

Received: 06/06/2026; Revised: 21/07/2026; Accepted: 27/07/2026; Published: 13/08/2026

The apparent pseudo-first-order model was selected for kinetic analysis based on several considerations. First, under the experimental conditions employed, hydrogen peroxide was maintained in stoichiometric excess relative to phenol (phenol concentration: 25 mg L^{-1}, H_2O_2 concentration: up to 30 mM). Under such conditions, the concentration of the oxidant remains effectively constant throughout the reaction, satisfying the pseudo-first-order assumption. Second, the use of a well-mixed slurry with fine catalyst particles (as confirmed by SEM) ensures that external mass transfer limitations are minimized, allowing the intrinsic surface reaction kinetics to be rate-determining.

This approach is designed as a practical comparative metric for process intensification rather than a comprehensive mechanistic rate law. The pseudo-first-order model provides a single apparent rate constant (K_{app}) that integrates the contributions of radical generation, adsorption, and surface reaction, enabling straightforward comparison of different operating conditions. While more complex models (e.g., Langmuir-Hinshelwood, Eley-Rideal, or Mars-van Krevelen) could provide more mechanistic detail, they require extensive experimental data including adsorption isotherms, competitive adsorption effects, and intermediate product distributions, which are beyond the scope of this initial kinetic study.

The simplicity of the pseudo-first-order model also facilitates practical engineering applications, such as reactor design and scale-up calculations, where a lumped rate constant is often sufficient for preliminary process evaluation.

3.0 Results and Discussion

3.1 Catalyst characterizations

The characterization results confirm that the impregnation-calcination route successfully generated an active CuO phase on the alumina support while largely preserving the textural integrity of the parent material. The XRD patterns of the γ-Al_2O_3 support and 9Cu/A catalyst are presented in Figure 1. The support exhibited characteristic diffraction peaks at 2θ = 25.54°, 35.17°, 37.80°, 43.37°, 57.55°, and 66.45°, corresponding to the (111), (200), (220), (311), (400), and (511) planes of γ-Al_2O_3, respectively [13]. These reflections confirm the presence of a well-crystallized cubic spinel structure typical of transition alumina phases.

Following impregnation with 9 wt% CuO, additional peaks were observed at 2θ = 35.4°, 38.7°, and 48.8°, which are characteristic of the (-111), (111), and (-202) planes of monoclinic CuO (tenorite) [14]. The relatively low intensity of these CuO reflections, compared to the alumina support peaks, indicates moderate copper loading and satisfactory dispersion of the active phase on the support surface [15]. Importantly, no peaks corresponding to copper-aluminate ($CuAl_2O_4$) or other mixed oxide phases were detected, suggesting that the calcination temperature of 600 °C was sufficient to form the CuO phase while avoiding undesirable solid-state reactions that could deactivate the catalyst. The preservation of the alumina structure after impregnation and calcination confirms the stability of the support under the preparation conditions.

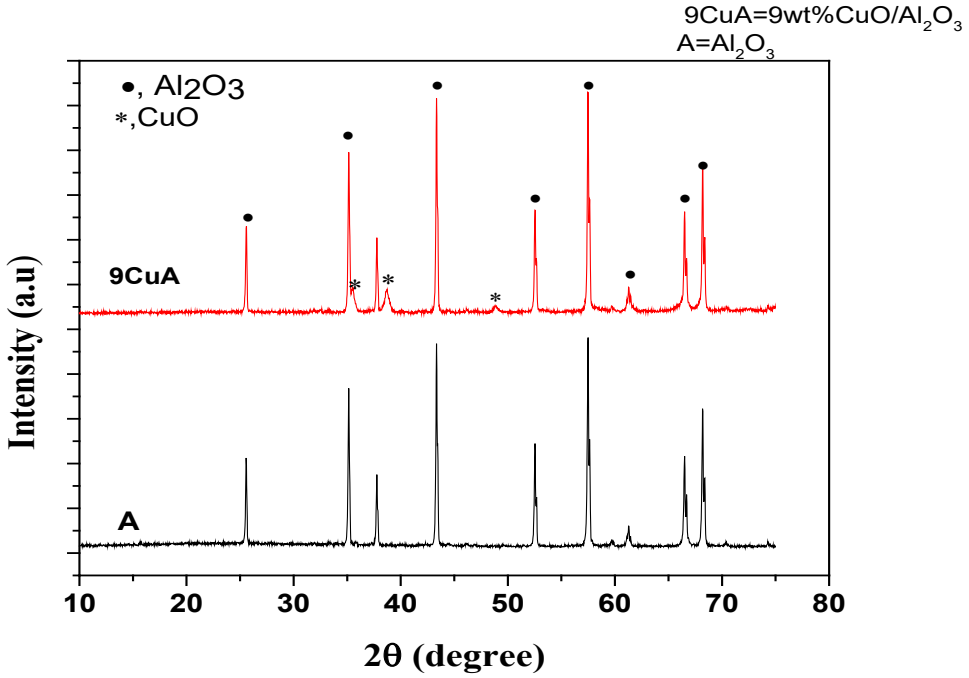

Figure 1: XRD patterns of the synthesized catalyst and support

Received: 06/06/2026; Revised: 21/07/2026; Accepted: 27/07/2026; Published: 13/08/2026

The textural properties of the support and catalyst are summarized in Table 1. The γ-Al_2O_3 support exhibited a specific surface area of 464.9 $m^2 g^{-1}$, pore volume of 0.422 $cm^3 g^{-1}$, and average pore diameter of 2.92 nm, characteristic of mesoporous alumina with a well-developed pore network. After CuO loading, the surface area increased slightly to 471.3 $m^2 g^{-1}$, while the pore volume remained essentially unchanged (0.425 $cm^3 g^{-1}$) and the average pore diameter decreased marginally to 2.80 nm. The slight increase in surface area can be attributed to several factors. First, the impregnation and subsequent calcination may have created additional surface roughness or microporosity through the decomposition of copper nitrate precursor, which releases gases (NO_x) during thermal treatment that can etch the alumina surface and generate new pores [16]. Second, the formation of highly dispersed CuO crystallites on the alumina surface can contribute to the measured surface area, particularly if the CuO particles are in the nanometer size range with high specific surface area [17]. Third, the calcination process may have completed the dehydration/dehydroxylation of the alumina surface, potentially exposing additional surface area that was previously occupied by hydroxyl groups or physisorbed water.

The minimal change in pore volume and the slight decrease in pore diameter suggest that CuO deposition occurred predominantly on the external surface and within the mesopores without significant pore blockage. The preservation of over 95% of the original pore volume indicates that the active phase is well-dispersed and accessible, which is favorable for catalytic applications where mass transport of reactants to active sites is critical [16].

The surface morphology of the γ-Al_2O_3 support and 9Cu/A catalyst was examined by SEM (Figure 2). The bare alumina (Figure 2A) exhibited closely packed irregular particles with a relatively smooth surface texture and a broad size distribution ranging from approximately 1-10 μm. The particles showed angular to sub-angular morphology characteristic of γ-Al_2O_3 derived from boehmite precursors. In contrast, the 9Cu/A catalyst (Figure 2B) revealed the presence of brighter, dispersed features on the alumina surface, which are attributed to CuO species. These features appear as small crystallites or clusters with sizes ranging from approximately 50-200 nm, uniformly distributed across the support surface. The brighter contrast in SEM backscattered electron images is consistent with the higher atomic number of copper (Z=29) compared to aluminum (Z=13), confirming the presence of copper-containing species on the surface.

Importantly, the dispersion appears relatively uniform, with no evidence of large CuO agglomerates or separate copper oxide particles. This observation is consistent with the XRD results, which indicated moderate copper loading and good dispersion, and with the BET results, which showed preserved porosity. The uniform distribution of CuO nanoparticles on the alumina support is critical for catalytic performance, as it maximizes the number of accessible active sites and prevents mass transfer limitations that would occur with larger agglomerates [17].

While FTIR analysis was not performed in this study, the combination of XRD, BET, and SEM characterization provides sufficient information about the catalyst structure, phase composition, textural properties, and morphology to support the catalytic performance discussion. The XRD patterns clearly confirm the presence of CuO phase and the absence of copper-aluminate formation, while the BET data demonstrate preserved porosity, and SEM reveals uniform dispersion of the active phase.

Table 1: Properties of the synthesized samples

Sample	Color	Surface area (m^2/g)	Pore volume (cm^3/g)	Average pore diameter (nm)
A	White	464.948	0.422	2.92
9Cu/A	Ash	471.270	0.425	2.80

Received: 06/06/2026; Revised: 21/07/2026; Accepted: 27/07/2026; Published: 13/08/2026

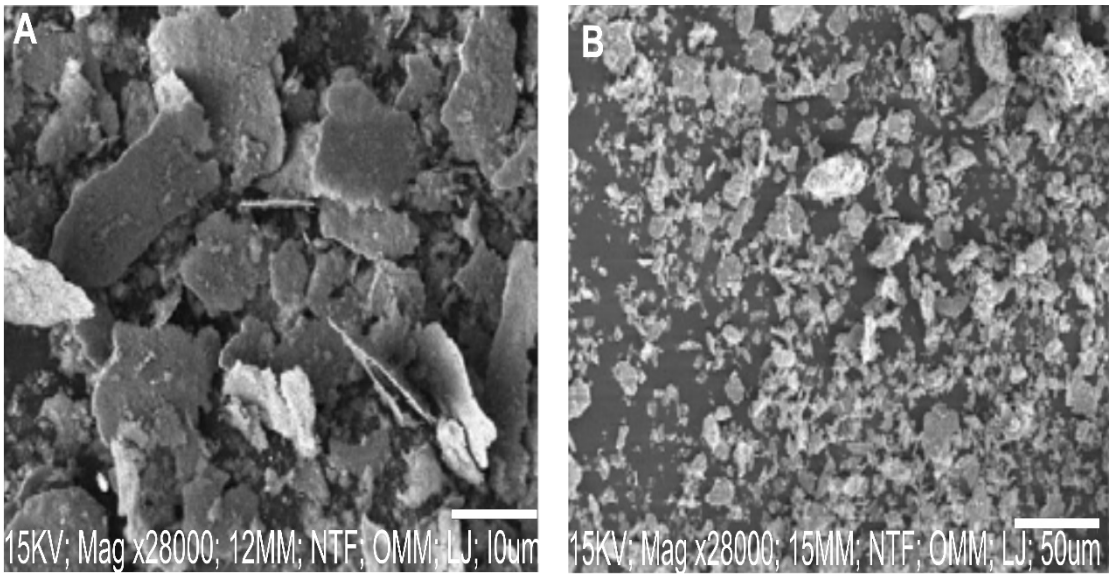

Figure 2: SEM images of the Al_2O_3 support (A) and the synthesized CuO/Al_2O_3 catalyst (B).

3.2 Degradation with ultrasound only

Figure 3 presents the response of phenol to ultrasonic irradiation alone. Degradation increased gradually over time, reaching approximately 8 % after 100 min. This low conversion aligns with the hydrophilic nature of phenol and the limited radical flux produced by sonolysis without additives [7]. These results confirm that ultrasound alone is insufficient for rapid phenol degradation and that process intensification may requires the addition of a catalyst, an oxidant, or both [18].

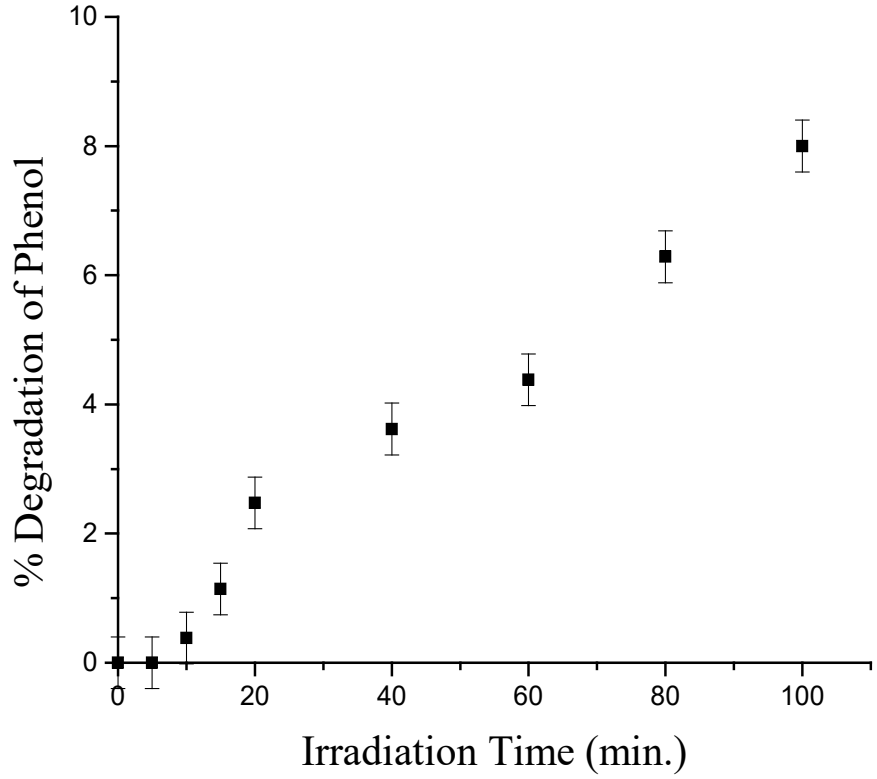

Figure 3. Effect of sonication time on phenol degradation during sole sonolysis at 25 °C and initial pH 6.3

3.3 Effect of oxidant concentration and catalyst dosage

Figure 4(a) illustrates the effect of H_2O_2 concentration. In the absence of H_2O_2 but with 20 g/L 9Cu/A, phenol removal reached 22.7 % after 100 minutes of irradiation, which is substantially higher than that observed for sonolysis alone. This result indicates that the catalyst facilitates interfacial radical generation and enhances

Received: 06/06/2026; Revised: 21/07/2026; Accepted: 27/07/2026; Published: 13/08/2026

adsorption activation [9]. The introduction of H_2O_2 markedly improved degradation efficiency, increasing from 22.7 % to a maximum of about 90 % at 30 mM. This enhancement is attributed to the catalytic and sonochemical decomposition of H_2O_2 into hydroxyl radicals [9]. However, the degradation dropped by 6.5 % as the H_2O_2 rose to 50 mM. This implies that hydrogen peroxide acts as a source of free radicals (equation (4) & (6)) which promotes phenol degradation and acts as a scavenger (equation (7)) of the free radicals produced at high concentrations, leading to the formation of less reactive species such as hydroperoxyl radicals, therefore, lowering the effective radical concentration available for phenol oxidation [19]. Thus, the observed drop in phenol degradation. The reactions pathway occurring in the presence of an external oxidant (H_2O_2) can be described as follows:

Interaction with the catalyst

$$Cu^{2+} + H_2O_2 \leftrightarrow Cu(OOH)^+ + H^+ \quad (2)$$

$$Cu(OOH)^+ \rightarrow Cu^+ + HO_2^{\bullet} \quad (3)$$

$$Cu^+ + H_2O_2 \rightarrow Cu^{2+} + HO^- + HO^{\bullet} \quad (4)$$

$$Cu^{2+} + HO_2^{\bullet} \rightarrow Cu^+ + H^+ + O_2 \quad (5)$$

Interaction with ultrasound

$$H_2O_2 +))) \rightarrow HO^{\bullet} + HO^- \quad (6)$$

$$HO^{\bullet} + H_2O_2 \rightarrow HO_2^{\bullet} + H_2O \quad (7)$$

$$HO_2^{\bullet} + H_2O_2 \rightarrow HO^{\bullet} + H_2O + O_2 \quad (8)$$

$$HO^{\bullet} + HO_2^{\bullet} \rightarrow H_2O + O_2 \quad (9)$$

$$2HO^{\bullet} \rightarrow H_2O + O^{\bullet} \quad (10)$$

Catalyst dosage exhibited a similar optimal trend, as shown in Figure 4(b). Increasing the 9Cu/A loading from 0 to 20 g/L consistently increased phenol conversion to approximately 90%, reflecting a greater number of active sites for H_2O_2 activation and an expanded interfacial area for phenol adsorption [20]. Beyond 20 g/L, degradation efficiency declined slightly. This behavior is commonly attributed to attenuation and scattering of the ultrasonic field by excess suspended solids, which reduces cavitation efficiency [21].

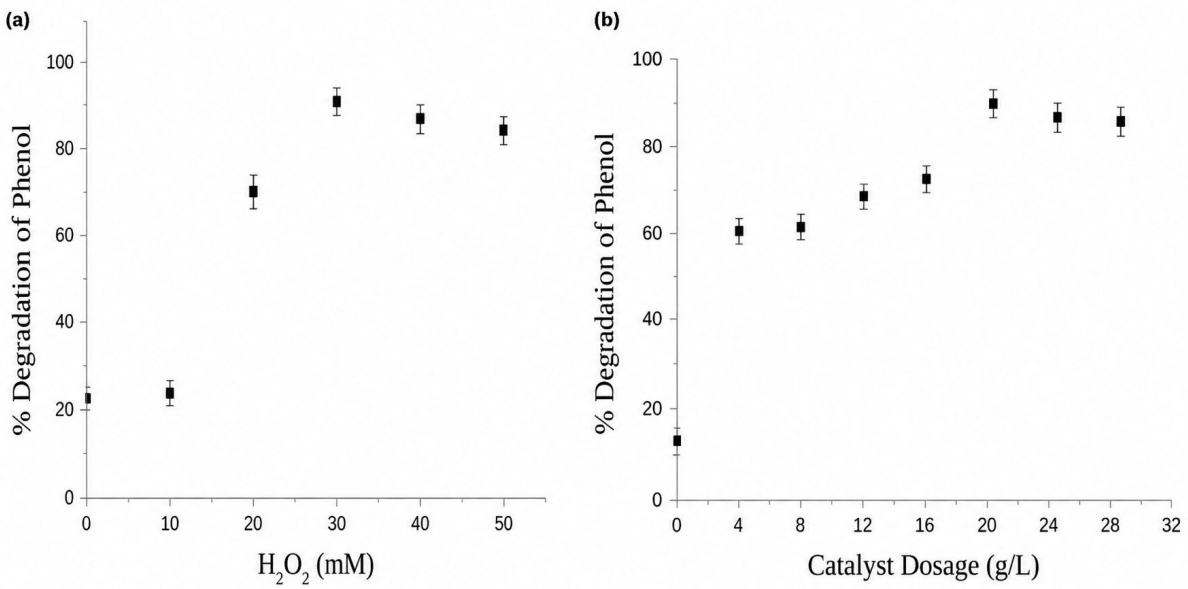

Figure 4: Effect of (a) H_2O_2 concentration and (b) catalyst dosage on phenol degradation over 9Cu/A after 100 min of sonication.

3.4 Influence of initial pH and temperature

The influence of solution pH (initial) on the level of phenol degradation has been explored by performing a series of experiments in the pH range of 4 to 6. All experimental runs used a fixed temperature of 50 °C, 30 mM H_2O_2, and a catalyst dosage of 20 g/L (9Cu/A). Figure 5(a) shows the obtained results. The figure shows that phenol degradation generally increased with decreasing pH, with the maximum degradation observed at pH 4. This higher degradation rate observed at lower pH value can be ascribed to the fact that the chemical nature of some organic contaminants in aqueous solution and the ionic properties of many catalyst active sites depend on solution pH [22]. Generally, at higher acid concentrations (lower pH), phenol in aqueous solution exists predominantly in its molecular form [23].

Received: 06/06/2026; Revised: 21/07/2026; Accepted: 27/07/2026; Published: 13/08/2026

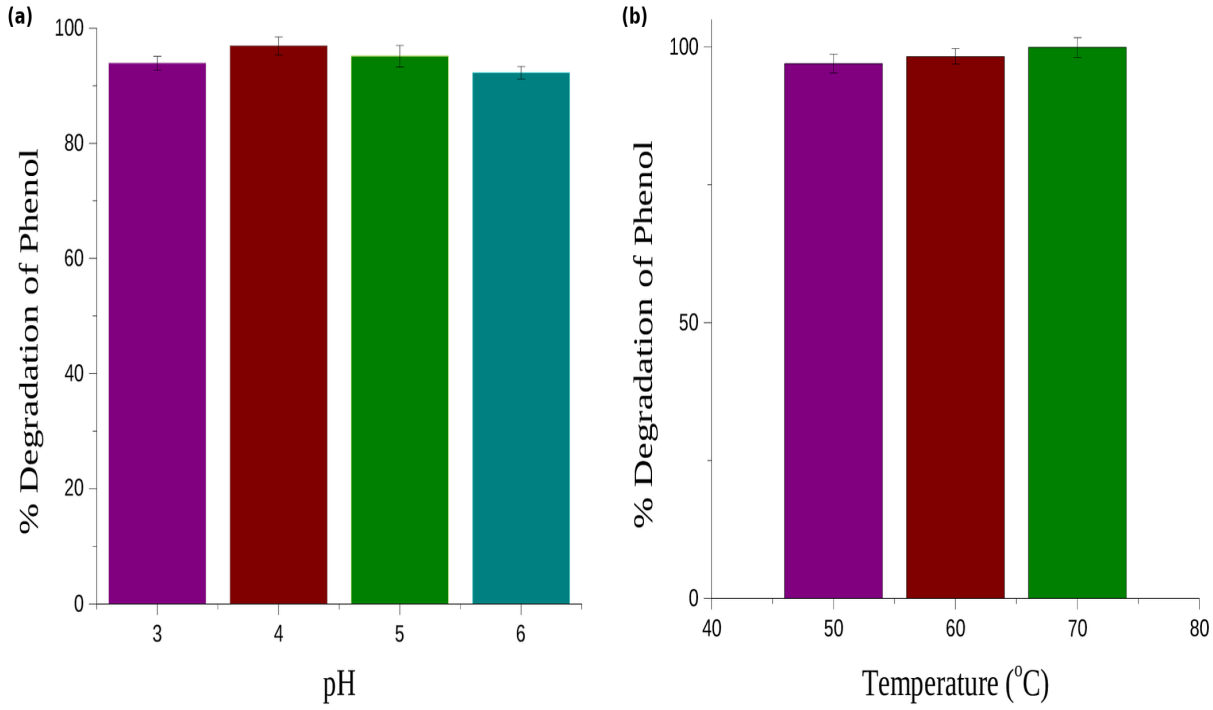

Figure 5: Effect of (a) initial pH and (b) temperature on phenol degradation over 9Cu/A after 100 min of sonication.

The effect of temperature, as shown in Figure 5(b), was relatively modest over the 50-70 °C range. Phenol removal remained consistently high throughout this interval, improving only slightly as the temperature increased. This limited response is characteristic of sonochemical oxidation, where elevated liquid temperatures can accelerate reaction kinetics but also reduce cavitation intensity due to increased vapor content within collapsing bubbles [24].

3.5 Kinetic Model

The phenol degradation kinetics were analyzed using a pseudo-first-order model (valid when the oxidant is in excess and mass transfer is not limiting). The first-order behavior as shown by the following equations (11-15). The apparent rate constant (K_{app}) was determined from the slope. For 9Cu/A (25 mg/L initial phenol, 100 min, 70 °C, pH 4, 30 mM H_2O_2), $K_{app} \approx 0.0331$ min^{-1}. Without a catalyst (sonolysis + H_2O_2 only), K_{app} was only ~0.0008 min^{-1}. These results strongly suggest that catalytic activation of H_2O_2 contributes significantly to $HO^{\bullet}$ generation (reaction (4)) rather than the mere sonication process (reaction (1)). This is consistent with literature reports that solid catalysts can dramatically accelerate advanced oxidation rates [7].

$$Phenol + [HO^{\bullet}] \rightarrow intermediate \rightarrow products \quad (11)$$

$$-r_{phenol} = \frac{d[Phenol]}{dt} = k[HO^{\bullet}][Phenol] \quad (12)$$

$HO^{\bullet}$ is assumed to be at a virtually constant value, that is, considering $[HO^{\bullet}]$ at a pseudo-steady-state condition [24].

The kinetic equation can be represented as:

$$-\frac{dC}{dt} = -r = k[HO^{\bullet}][Phenol] = K_{app}[Phenol] \quad (13)$$

Where "C" is the concentration, "r" is the reaction rate, "k" is the kinetic reaction rate constant, and "K_{app}" is the apparent pseudo-first order kinetic constant.

$$\frac{d[Phenol]}{[Phenol]} = K_{app}dt = \frac{dC}{C} \quad (14)$$

Integrating equation (14) within the time interval of [0, t]

$$\ln\frac{C_t}{C_0} = -K_{app}t \quad (15)$$

[24]

Received: 06/06/2026; Revised: 21/07/2026; Accepted: 27/07/2026; Published: 13/08/2026

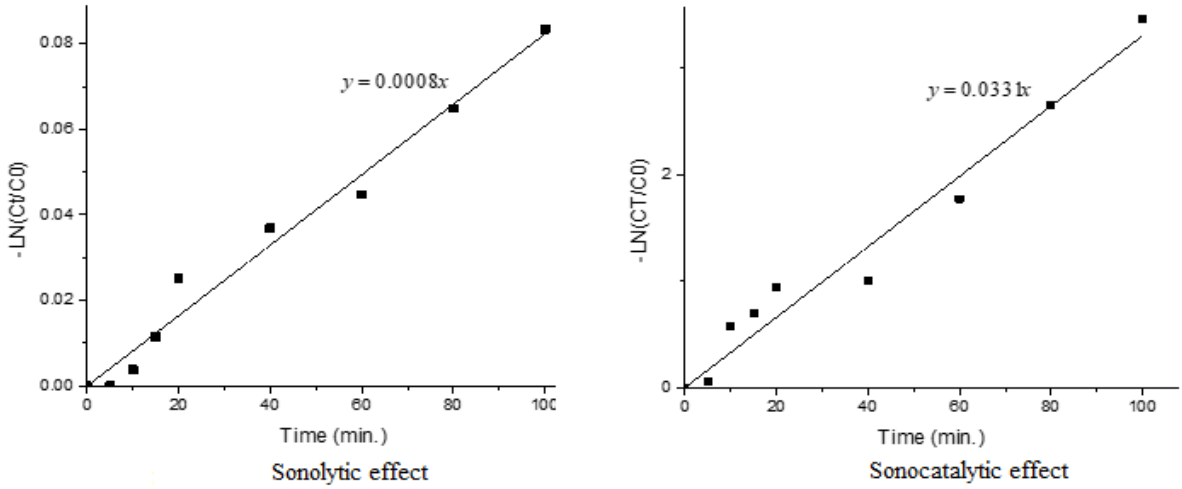

Figure 6: First order kinetic model of the degradation of phenol using 9Cu/A catalyst

The choice of pseudo-first-order kinetic analysis is justified by the experimental conditions. The high H_2O_2-to-phenol molar ratio (approximately 1200:1 at 30 mM H_2O_2 and 25 mg L^{-1} phenol) ensures that oxidant concentration remains effectively constant during the reaction. Additionally, the use of 20 g L^{-1} catalyst with fine particle dispersion (as confirmed by SEM) minimizes mass transfer limitations, making surface reaction the rate-determining step. Previous studies on similar sonocatalytic systems have also successfully employed pseudo-first-order kinetics for comparative analysis of degradation efficiency [7,24].

The linear correlation coefficients ($R^2 > 0.98$) obtained for all experimental conditions confirm the validity of the pseudo-first-order assumption. A zero-order, and Second-order models were also tested but showed poor correlations of $R^2 < 0.85$, and $R^2 < 0.89$ respectively, confirming that the reaction is first-order with respect to phenol concentration under the conditions studied.

4.0 Conclusion

The 9 wt% CuO/Al_2O_3 catalyst was successfully synthesized by incipient-wetness impregnation and applied in the sonocatalytic degradation of phenol. Characterization by XRD, BET, and SEM confirmed that CuO was deposited on the alumina support without severe loss of textural properties. The catalyst retained high surface area, stable pore volume, and accessible active sites, which supported its role in interfacial oxidation reactions.

Phenol degradation under ultrasound alone was poor, with only about 8 % removal after 100 min. The presence of 9Cu/A increased degradation, while the combined use of ultrasound, catalyst, and H_2O_2 produced the best result. Maximum phenol removal of about 90 % was obtained at 30 mM H_2O_2, 20 g/L catalyst dosage, pH 4, and elevated reaction temperature. Higher H_2O_2 concentration lowered performance due to hydroxyl radical scavenging, while excess catalyst reduced cavitation efficiency through ultrasonic wave shielding and particle scattering.

The degradation data followed an apparent pseudo-first-order kinetic model. The apparent rate constant reached about 0.0331 min^{-1} under optimal catalytic conditions, far higher than the value obtained for sonolysis with H_2O_2 in the absence of catalyst. This confirms that CuO/Al_2O_3 actively promotes H_2O_2 decomposition and hydroxyl radical generation during ultrasound-assisted oxidation. The study therefore establishes 9Cu/A as an effective catalyst for phenol degradation and provides a useful kinetic baseline for future optimization of CuO/Al_2O_3-based sonocatalytic wastewater treatment systems.

References

[1] A. Devard, P. Brussino, F. A. Marchesini, and M. A. Ulla, "Cu(5%)/Al_2O_3 catalytic performance on the phenol wet oxidation with H_2O_2: Influence of the calcination temperature," *J. Environ. Chem. Eng.*, vol. 7, no. 4, p. 103201, Aug. 2019, doi: 10.1016/j.jece.2019.103201.

[2] Z. Guerra-Que, H. Pérez-Vidal, G. Torres-Torres, J. Carlos Arévalo-Pérez, A. A. S. Pavón, A. Cervantes-Uribe, A. E. Monteros, M. Antonia Lunagómez-Rocha, "Treatment of phenol by catalytic wet air oxidation: a comparative study of copper and nickel supported on γ-alumina, ceria and γ-alumina–ceria," RSC Adv., vol. 9, no. 15, pp. 8463–8479, 2019, doi: 10.1039/C9RA00509A.

[3] A. S. Hadi Ghazvini, A. Khataee, M. Fathinia, H. Haghighat, and N. Kudaibergenov, "Sonocatalytic degradation of furazolidone using a heterogeneous triple ion synergy system of ZnFe2O4@ZIF-67

Received: 06/06/2026; Revised: 21/07/2026; Accepted: 27/07/2026; Published: 13/08/2026

nanostructures: Physicochemical Characterization and degradation pathway," *Chem. Eng. J.*, vol. 501, p. 157273, Dec. 2024, doi: 10.1016/j.cej.2024.157273.

[4] Y. Ma, Zhou, Y, Wen, N, Gu, Q, Chen, M, Zhang, Y, Xie, J, He, M, "Unraveling the structural and pH-dependent inhibitory mechanisms of phenolic fractions in dissolved organic matter on the degradation of aromatic disinfection byproducts by the UV/PAA process," *Sep. Purif. Technol.*, vol. 381, p. 135645, Feb. 2026, doi: 10.1016/j.seppur.2025.135645.

[5] T. Shende, G. Andaluri, and R. P. S. Suri, "Kinetic model for sonolytic degradation of non-volatile surfactants: Perfluoroalkyl substances," *Ultrason. Sonochem.*, vol. 51, pp. 359–368, Mar. 2019, doi: 10.1016/j.ultsonch.2018.08.028.

[6] F. A. Aderibigbe, A. A. Adelanke, S. I. Mustapha, T. L. Adewoye, K. B. Muritala, R. B. Abdulafeez, "Phenol removal from refinery wastewater: A review of biosorption technologies," *Res.*, vol. 5, p. 101297, Mar. 2026, doi: 10.1016/j.nexres.2025.101297.

[7] J. Madhavan, J. Theerthagiri, D. Balaji, S. Sunitha, M. Y. Choi, and M. Ashokkumar, "Hybrid Advanced Oxidation Processes Involving Ultrasound: An Overview," *Molecules*, vol. 24, no. 18, p. 3341, Sep. 2019, doi: 10.3390/molecules24183341.

[8] P. Qiu, B. Park, J. Choi, B. Thokchom, A. B. Pandit, and J. Khim, "A review on heterogeneous sonocatalyst for treatment of organic pollutants in aqueous phase based on catalytic mechanism," *Ultrason. Sonochem.*, vol. 45, pp. 29–49, 2018, doi: 10.1016/j.ultsonch.2018.03.003.

[9] B. Y. Jibril and A. Y. Atta, "Journal of Industrial and Engineering Chemistry Effect of copper loadings on product selectivities in microwave- enhanced degradation of phenol on alumina-supported copper oxides," *J. Ind. Eng. Chem.*, vol. 19, no. 6, pp. 1800–1804, 2013, doi: 10.1016/j.jiec.2013.02.023.

[10] S.-K. Kim, K.-H. Kim, and S.-K. Ihm, "The characteristics of wet air oxidation of phenol over CuO_x/Al_2O_3 catalysts: Effect of copper loading," *Chemosphere*, vol. 68, no. 2, pp. 287–292, Jun. 2007, doi: 10.1016/j.chemosphere.2006.12.080.

[11] J. Yu and P. E. Savage, "Phenol oxidation over CuO/Al2O3 in supercritical water," *Appl. Catal. B Environ.*, vol. 28, no. 3, pp. 275–288, Dec. 2000, doi: 10.1016/S0926-3373(00)00184-3.

[12] M. J. Angeles-Hernández, G. A. Leeke, and R. C. D. Santos, "Catalytic Supercritical Water Oxidation for the Destruction of Quinoline Over MnO_2/CuO Mixed Catalyst," *Ind. Eng. Chem. Res.*, vol. 48, no. 3, pp. 1208–1214, Feb. 2009, doi: 10.1021/ie8006402.

[13] A. Boumaza, A. Djelloul, and F. Guerrab, "Specific signatures of α-alumina powders prepared by calcination of boehmite or gibbsite," *Powder Technol.*, vol. 201, no. 2, pp. 177–180, 2010, doi: 10.1016/j.powtec.2010.03.036.

[14] W. Pan, G. Zhang, T. Zheng, and P. Wang, "Degradation of p-nitrophenol using CuO/Al_2O_3 as a Fenton-like catalyst under microwave irradiation," *RSC Adv.*, vol. 5, no. 34, pp. 27043–27051, 2015, doi: 10.1039/c4ra14516j.

[15] Y. Bai, X. Bian, and W. Wu, "Applied Surface Science Catalytic properties of CuO / CeO_2-Al_2O_3 catalysts for low concentration NO reduction with CO," *Appl. Surf. Sci.*, vol. 463, no. August 2018, pp. 435–444, 2019, doi: 10.1016/j.apsusc.2018.08.229.

[16] W. W. Wang, W. Z. Yu, P. P. Du, H. Xu, Z. Jin, R. Si, C. Ma, S. Shi, C. J. Jia, C. H. Yan, "Crystal Plane Effect of Ceria on Supported Copper Oxide Cluster Catalyst for CO Oxidation: Importance of Metal – Support," 2017.

[17] S. M. Anisuzzamana, A. Bonob, D. Krishnaiahb, F. A. Lahinb, and C. Ramlanb, "Characterization of Different Metal Oxide Promoted Alumina Catalyst," *Borneo Sci. J. Sci. Technol.*, vol. 38, no. 2, 2017, doi: 10.51200/bsj.v38i2.4412.

[18] Y. Segura, F. Martínez, J. A. Melero, R. Molina, R. Chand, and D. H. Bremner, "Enhancement of the advanced Fenton process (Fe 0/H 2O 2) by ultrasound for the mineralization of phenol," *Appl. Catal. B Environ.*, vol. 113–114, pp. 100–106, 2012, doi: 10.1016/j.apcatb.2011.11.024.

[19] L. Covinich, F. Felissia, P. Massa, R. Fenoglio, and M. C. Area, "Kinetic modeling of a heterogeneous Fenton - type oxidative treatment of complex industrial effluent," *Int. J. Ind. Chem.*, vol. 9, no. 3, pp. 215–229, 2018, doi: 10.1007/s40090-018-0151-6.

[20] H. Su, Y. Xie, X. Cheng, Z. Yang, J. Mao, H. Yang, X. Xu, S. Pan, H. Hu, "The effect of dual-frequency ultrasound on synergistic Sonochemical oxidation to degrade aflatoxin B1," *Food Chem.*, vol. 457, p. 139708, Nov. 2024, doi: 10.1016/j.foodchem.2024.139708.

[21] G. M. S. Elshafei, F. Z. Yehia, O. I. H. Dimitry, A. M. Badawi, and G. Eshaq, "Ultrasonic assisted-Fenton-like degradation of nitrobenzene at neutral pH using nanosized oxides of Fe and Cu," *Ultrason. Sonochem.*, vol. 21, no. 4, pp. 1358–1365, 2014, doi: 10.1016/j.ultsonch.2013.12.019.

[22] W. Pan, G. Zhang, T. Zheng, and P. Wang, "Degradation of p-nitrophenol using CuO/Al<inf>2</inf>O<inf>3</inf> as a Fenton-like catalyst under microwave irradiation," *RSC Adv.*, vol. 5, no. 34, pp. 27043–27051, 2015, doi: 10.1039/c4ra14516j.

[23] S. Sedaghat, "Ultrasonic decomposition of organic compounds in wastewater," *Asian J. Chem.*, vol. 24, no. 10, pp. 4815–4816, 2012.
[24] F. Z. Yehia, G. Eshaq, A. M. Rabie, A. H. Mady, and A. E. Elmetwally, "Phenol degradation by advanced Fenton process in combination with ultrasonic irradiation," *Egypt. J. Pet.*, vol. 24, no. 1, pp. 13–18, 2015, doi: 10.1016/j.ejpe.2015.03.002.

Received: 06/06/2026; Revised: 21/07/2026; Accepted: 27/07/2026; Published: 13/08/2026